EVALUATION OF WATER EVAPORATION AND SALT PRECIPITATION DUE TO FLOW IN GAS RESERVOIRS

Carlos Grattoni[a], Phil Guise[a], Graham Phillips[a], Quentin Fisher[b] and Rob Knipe[a]

a Rock Deformation Research Ltd, University of Leeds, LS2 9JT, UK

b School of Earth and the Environment, University of Leeds, LS2 9JT, UK

This paper was prepared for presentation at the International Symposium of the Society of Core Analysts held in Noordwijk, The Netherlands 27-30 September, 2009

ABSTRACT

Gas reservoirs usually produce some associated water during gas production. Within the reservoir, mainly near the well bore, water evaporates as the reservoir pressure declines, and the partial water pressure increases. Water evaporation also occurs in gas reservoirs when dry gas is injected for pressure maintenance or CO_2 sequestration. Water vaporization concentrates mineral components in the brine, and in high salinity brines can induce mineral precipitation inducing loss of injectivity and productivity. Several field cases have been reported where precipitation of halite is believed to be the cause of formation damage and it has been usually associated with water vaporisation. The aim of this paper is to gain an improved understanding of water evaporation and salt precipitation associated with the gas flow within sandstone reservoirs.

Experiments were conducted to evaluate the rate of water vaporization and amount of salt precipitation caused by the flow of dry methane through North Sea core plugs containing high salinity brine at irreducible water saturation. The initial brine distribution as well as the movement of the evaporation front (gas saturation evolution) within the core has been evaluated by using CT scanning. The mass of water produced was also verified by monitoring the amount of water adsorbed from the effluent gas.

The measurement of water content of the produced gas shows a constant and a falling rate of vaporization. The vaporization process results in halite drop-out which was evaluated by total and component material balance. The saturations become difficult to evaluate during water vaporization due to the variation of brine salinity, the precipitation of salt and reduction of the pore space. In-situ saturation determination with CT scanning improves the understanding of the vaporisation process and the calculation of saturations. Experimental results indicate that not all the water in the brine can be evaporated, which can be interpreted as an increase in capillary pressure and a reduction of vapour pressure due to increased brine salinity.

INTRODUCTION

Water vaporization due to gas flow often occurs in gas reservoirs under a wide range of conditions such as depletion in high pressure-temperature reservoirs, near wellbore during methane storage in depleted reservoirs, and as a mechanism inducing sub-capillary equilibrium water saturations in tight gas reservoirs [1]. During production,

water vaporization occurs due to the increase in water partial pressure, as the reservoir gas pressure declines in the vicinity of the well bore. When gas reservoirs are used for temporary gas storage dry gas is injected which also vaporises water as it flows through the rock, both near the well bore and deeper in the reservoir. The water moisture content in the gas is a function of pressure; temperature, gas velocity and brine salinity. Vaporisation of the brine reduces water saturation increasing the effective gas mobility. However, water vaporization concentrates mineral components in the brine, and in high salinity brines can induce mineral precipitation within the formation, which will increase over time leading to a reduction in gas permeability. The form or type of the deposited salt will depend on the extent of brine super-saturation achieved.

In reservoirs containing high salinity brines Halite precipitation may cause loss of injectivity, productivity and eventually may lead to salt plugging. Prediction of the amount of damage and decrease in production has been reported [1,2,3]. In spite of being an important problem not much research has been performed in this area. Zuluaga and co-authors [4, 5, 6] have produced a series of semi-analytical and numerical models that describe the vaporisation process under a wide range of conditions. However, to our knowledge the saturation distribution and traveling wave through the rock has not been verified experimentally.

The main aim of this paper is to improve the understanding of the processes involved during water vaporisation and salt precipitation. In order to achieve this objective a series of laboratory experiments were undertaken.

EXPERIMENTAL METHODOLOGY

Experiments were performed in a model system using methane flow through a high permeability North Sea sandstone and synthetic brine.

Samples

The rock is Permian reservoir sandstone, of aeolian origin, which is part of the Rotliegend Sandstone Group. The core plugs were scanned using an X-ray computer tomography (CT) system to identify their homogeneity and integrity. Thin parallel laminations, which are characteristic of this reservoir rock, can be clearly observed in the CT images – Figure 1. The NMR T2 distribution confirms the presence of a wide range of pore sizes. The gas-brine drainage capillary determined with a centrifuge is also shown in Figure 1. All the core plugs were cleaned by Soxhlet extraction with toluene/methanol and dried before being tested. The core plugs have 13 -15 % porosity and a Klinkenberg permeability of 50 - 200 md. Brine containing 20% NaCl (degassed and filtered through 0.45 μm) was used to saturate the cores. Due to space limitations only one vaporisation experiment, denoted B12, will be reported here. The core plug used in this experiment has a porosity of 14.1% and a permeability of 50.7 mD at an effective stress of 2000 psi. Before starting the vaporisation experiment the core plug was drained to a low water saturation using the porous plate method with a capillary pressure of 180 psi.

Vaporisation Methodology

The schematic of the experimental set up used is shown in Fig. 2. The equipment comprises a composite X-ray transparent core-holder with internal heaters to keep the temperature constant. Two Quizix pumps, two methane gas accumulators and heated vessels are connected upstream of the coreholder. On the downstream side a backpressure regulator is connected to a desiccator on a balance (to absorb and determine the water vapor produced in the gas stream) and a gas flow meter. The experimental variables such as pressures, temperatures and weights were logged into a computer using Labview 7. The confining pressure was kept constant with a single piston flow pump in conjunction with a constant pressure control unit. Dry methane was injected at constant rate while the backpressure was kept constant. In-situ saturation profiles and mean saturation in all the cases have been obtained using X-ray CT scanning. The saturation calculations have been based on the gas phase and porosity distribution [7] as the brine changes its concentration (CT Number) during the experiment. Additionally, as the water evaporates the possible formation of salt crystals introduces a new solid phase.

RESULTS

Vaporisation experiment B12 is part of larger study and was performed at an average methane pressure of 2940 psi and a temperature of 45 ^{o}C. The pump flow rate was set at 0.1 cm^3/min, at ambient temperature and 2950 psi. This rate is equivalent to an average 1.0 scf/D or 1200 mol/m^2/day. The total amount of gas injected during this experiment was 81 pore volumes.

The porosity distribution and initial gas saturation along the length of the core calculated from CT data are shown in Figure 3. The average initial gas saturation was 78 %. The upstream pressure and cumulative volume of methane produced during vaporisation are shown in Figure 4. The figure also shows the gas molar flux. The oscillations in gas flux are due to inertia in the backpressure regulator introduces oscillation and variation.

The cumulative water production (Figure 5) shows two vaporisation regimes: (i) large initial vaporisation rate of 0.43 g/mol, up to an accumulative gas injected of 2 moles after ~ 31 hrs, followed by (ii) a decreasing rate of production until it becomes negligible after 7 moles of injected gas. It is possible that there is a change in the vaporisation mechanism between the two regimes, for example the brine becomes saturated with salt. It is worth noting that the produced water has been vaporised and therefore does not contain salt (i.e., distilled water).

A first approximation for calculating the water saturation can be obtained by assuming that all the salt remains in solution (no precipitation) and the density of the produced water and the water within the rock are the same. The average water saturation decreases as the vaporisation progresses (Figure 6), confirming a change of rate after 31 hours. The final (residual) brine saturation calculated using the above approximation is 8.0%.

In order to follow the vaporisation the gas saturation distribution and its evolution within the core, the front was evaluated using CT scanning, for more details see Appendix A. The evolution of the gas saturation profiles are shown in Figure 7. The

evaporation front reaches half length of the core at approximately 17 hours and the end of the core after 34 hours. The evaporation continues uniformly along the core between 34 and 137 hours. The average gas saturation at the end of the experiment is 91.0% (apparent brine saturation 9.0%).

DISCUSSION

A material balance on the brine components (water and salt) before and after the experiment, plus concentration and densities of brine solutions [8, 9] can be used to estimate the amount of salt precipitated and the brine saturation. Using this improved method of calculation for saturations the final water component saturation is 6.8 %, and a brine saturation of 7.8% is obtained, and the solid salt should fill 0.5 % of the pore space. Therefore the calculated gas saturation is 91.7 % which agrees very well with the saturation obtained using the CT data and the approximate calculation. This validates the assumption used in the CT calculations and the saturations profiles obtained.

In order to verify the location of the salt precipitation one end of the core was impregnated with epoxy and a sample was dry-cut (trimmed) for backscatter SEM. The sample was polished using ethane diol and propan-2-ol to avoid water dissolution of the precipitated salt. The SEM pictures, Figure 8, clearly show that the halite distribution is uneven. Halite is mostly located in the finest-grained layers where the pores are smallest; these are typically enriched in clays relative to coarser-grained layers and have experienced stronger chemical compaction. Although halite is very uncommon within the coarser-grained layers, it is present locally, typically adjacent to the halite-enriched layers. These observations indicate that before vaporisation the capillary bound water was mainly contained in the low permeability laminations while the gas was flowing through the high permeability lamina. The evaporation may have started in the boundary between lamina, so water was drawn do the lamina interface. In a similar way the crystallization progressed from the boundary into the fine grained zone. Different morphologies of crystals were found: the surface of some grains were covered by parallel flaked crystals, while the crystals are undistinguishable within the clays and very small pores, The later may be due to fast crystallization linked to extreme supersaturation.

Saturation distributions obtained by CT scans show that the initial high evaporation rate approximately ends when the vaporisation front reaches the outlet of the core; e.g., when the gas saturation starts to increase in the outlet end of the core. However, the gas does not seem to be in local equilibrium while water is still being vaporized as the gas saturation increases gradually along the length of the core. This indicates that the gas becomes gradually saturated as it flows through the sample. This observation contradicts the assumption of local thermodynamic equilibrium used in recent models of traveling waves [7]. The results also show that the start of the falling vaporisation rate is unrelated to the precipitation of minerals; as in one experiment our calculations indicated that salt was precipitated near the inlet before the vaporisation breakthrough.

During the decreasing vaporisation rate, or second regime, the gas saturation increases uniformly along the core indicating that the gas phase was vaporising water at approximately the same rate at different positions along the core. Previously [6] it was proposed that a moving capillary transition zone was responsible for this effect. Another

striking difference between our experiments and published models is that in none of the experiments the water saturation along the length of the core dropped to zero. This can be simply explained as water evaporates the brine becomes more concentrated and the water partial pressure drops which agrees with the predictions of Duan and Mao [10].

The initial, or constant vaporisation rate, depends on gas flow rate, initial water saturation, pressure and temperature. The experimental rate of water vaporisation ranged from 0.1 to 0.6 g of water per mol of methane. The rate of vaporisation at high pressure and low gas flow rate is more than double that at lower pressure and high flow rate. This may be due to local heterogeneities or at higher velocity not all the gas contacts the water lining the pore walls and therefore it requires more gas to evaporate the same amount of water. Extrapolation of this observation to reservoir conditions indicates that the vaporisation rate deep into the reservoir could double the rate compared to near wellbore conditions.

CONCLUSIONS

The water production experiments show an initial higher and constant rate of vaporisation, followed by a gradual decrease of water produced which qualitatively agrees with previous observations and recently published numerical models. The initial rate depends on gas flow rate, initial water saturation, pressure and temperature.

Water saturation is very difficult to evaluate during water vaporization due to the variation of brine salinity, the precipitation of salt and reduction of the pore space. In contrast gas saturation is unequivocal. In-situ saturation determination with CT scanning improves the understanding of the vaporisation process and the calculation of the different saturations.

Saturation distributions obtained by CT scans show that during the initial high rate period a diffuse evaporation front advances within the core. This period ends with the breakthrough of the vaporisation front. However, the gas does not seem to be in local equilibrium while water is still been evaporated. During the second regime with a decreasing vaporisation rate the gas saturation increases uniformly along the cores indicating that water is evaporating at an approximately uniform rate along the core.

In contrast to model predictions, the water production stopped for a dry gas injection, even when considerable amounts of water/brine was left in the pore space. The final brine saturation varied between 3 to 10 % in these experiments. Equilibrium calculations indicate that up to 2 % of the pore space could be occupied by precipitated salt and SEM images confirm these results.

The observations presented in this paper can contribute towards the design of surface production facilities for water separation and to improve the evaluation of tight gas reservoirs in the presence of high salinity brines.

ACKNOWLEDGEMENTS

The authors wish to express their gratitude to the following Sponsors for supporting the Sorby multiphase laboratory at the Univ. of Leeds: BP, BG Group, Chevron, Conoco Philips, Exxon Mobil, PDO, Petrobras, Shell, Statoil, and Total.

APPENDIX A

Gas Saturation determination using CT

Porosity at any point of the core can be determined from scans at the same position while the pore space is fully saturated with gas and brine. The porosity of each volume element can be calculated as:

$$\phi = \frac{CTrw - CTrg}{CTw - CTg} \tag{1}$$

Where ϕ is the porosity, CT is the CT number in Hounsfield Units, and the subscripts *g, r, w* refer to gas, rock and water respectively. The porosity as a function of length is calculated from the cross sectional area of each image, dry and saturated with KBr doped brine.

Traditionally water or gas saturation can be calculated from linear interpolation [11] between the dry and water saturated volume or slice:

$$Sw = \frac{CTsw - CTrg}{CTrw - CTrg} \tag{2}$$

where *CTsw is t*he CT number of the volume at a water saturation *Sw.* This is applicable when the *CTw* does not change during the experiment. However, during evaporation the brine concentration is continuously changing inducing a variable *CTrw*. Additionally, when salt is precipitated out of the brine the system has 2 solid and 2 fluid phases. Therefore, most of the methods used to calculate 3 phase saturations, such as linear interpolation, one immobile phase, dual energy scan or matched CT fluids, become inapplicable without any additional knowledge such as brine composition distribution. Approximate solutions can be obtained with the aid of other laboratory techniques such as measuring the total amount of water evaporated, then calculating the average brine composition and assuming that the composition is uniform along the length of the core. Our results clearly show that is a very crude approximation as there is a progressive evaporation along the length of the core.

Our approach is based on the knowledge of the porosity distribution under stress, which can be calculated using equation (1). Thus equation (1) and (2) can be combined and rearranged to obtain:

$$Sg\ (x) = \frac{1}{\phi(x)}\left(\frac{CTsg(x) - CTrg}{CTw - CTg}\right) \tag{3}$$

where *x* is a position along the length of the core and *CTsg* is the CT number of slice *x* a gas saturation *Sg*. In order to obtain reliable results the Ct images beam hardening must be minimized and the CT numbers of water and gas should be obtained inside the sleeve within the core holder. Additionally, reference materials are also used in every profile determination in order to correct for CT drifts.

REFERENCES

1. Newsham, K.E., Rushing, A. J, 2002. "Laboratory and Field Evaluation of an Apparent Sub-Capillary Equilibrium Water Saturation Distribution in a Tight Gas Sand" Reservoir. *SPE 75710*. SPE Gas Technology Symposium, Calgary, Canada. Search and Discovery Article # 40400 (2009): http://www.searchanddiscovery.net/documents/2009/40400newsham/index.htm

2. Jasinski, R., Sablerolle, W., Amory, M., 1997. "ETAP: Scale Prediction and Control for the Heron Cluster". *SPE 38767*. Annual Technical Conference and Exhibition, San Antonio, Texas. .

3. Graham, G. M., Jordan, M.M., Graham, G.C., Sablerolle, W., Hill. P, Bunney, J., 1997. "The implication of HP/HT Reservoir Conditions on the Selection and Application of Conventional Scale Inhibitors: Thermal Stability Studies". *SPE 37274*. Int. Symposium on Oilfield Chemistry, Houston, Texas.

4. Zuluaga, B., Munoz, N.I., Obando, G.A, 2001. "An Experimental Study to Evaluate Water Vaporisation and Formation Damage Caused by Dry Gas Flow through Porous Media". *SPE 68335***.**International Symposium on Oilfield Scale, Aberdeen, UK.

5. Zuluaga, E., Lake L.W., 2005. "Semi-Analytical Model for Water Vaporization in Gas Producers"**.** *SPE 93862*. Western Regional Meeting, Irvine, California.

6. Zuluaga, E., Lake L.W. "Modeling of Experiments on Water Vaporization for Gas Injection Using Traveling Waves". *SPE Journal,* (2008) **13**, 248-256.

7. Mees, F., Swennen, R. VanGeet, M., Jacobs, *Applications of X-ray computed tomography in the geosciences*. Published by Geological Society, London, 2003.

8. Ohe, S.,. "Prediction of Salt Effect on Vapor-Liquid Equilibria", *Fluid Phase Equilibria* (1998), **144**, 119-129.

9. Salt Institute (2008) http://www.saltinstitute.org/About-salt see Chemical and Physical properties. Last visited February 2009.

10. Duan, Z., Mao, S. A. "Thermodynamic Model for Calculating Methane Solubility, Density and Gas Phase composition of Methane-bearing Aqueous Fluids from 273 to 523K and From 1 to 2000 bar". *Geochemica et Cosmochimica Acta* (2006), **70**, 3369-3386.

11. Zisner, B. and Pellerin, F.M. (2007) A geoscientist's Guide to Petrophysics. Editions Technip, Paris, France. ISBN 9782710808992.

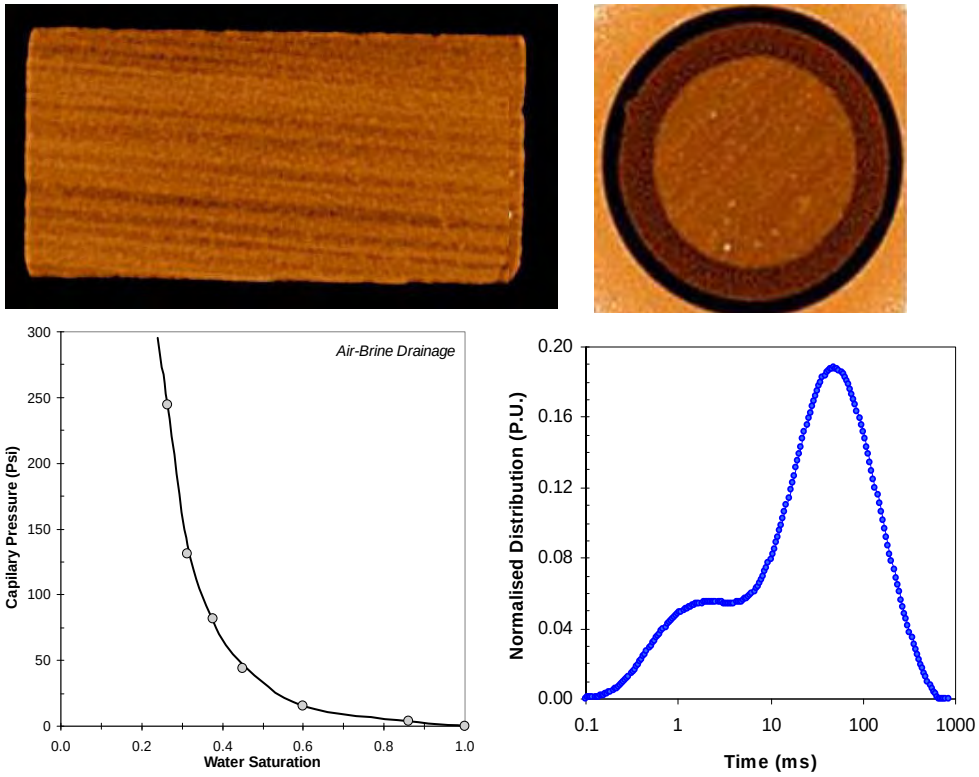

Figure 1 Sample Characterisation: NMR T2 distribution, X-ray CT imaging, gas-brine capillary pressure and SEM. The thin laminations along the core plug are characteristics of this formation.

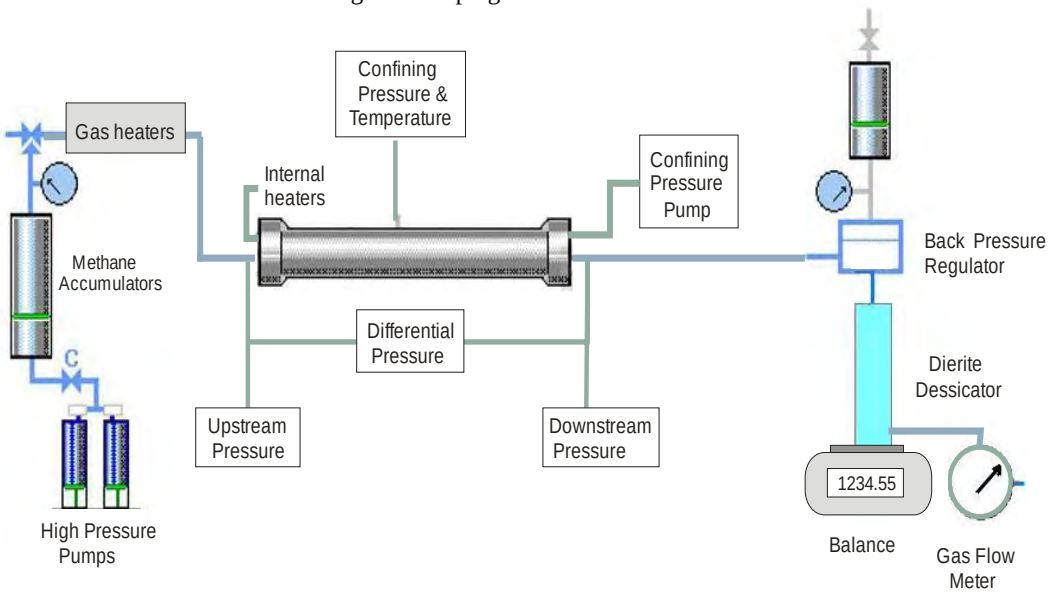

Figure 2- Schematic of the setup used for the water vaporization.

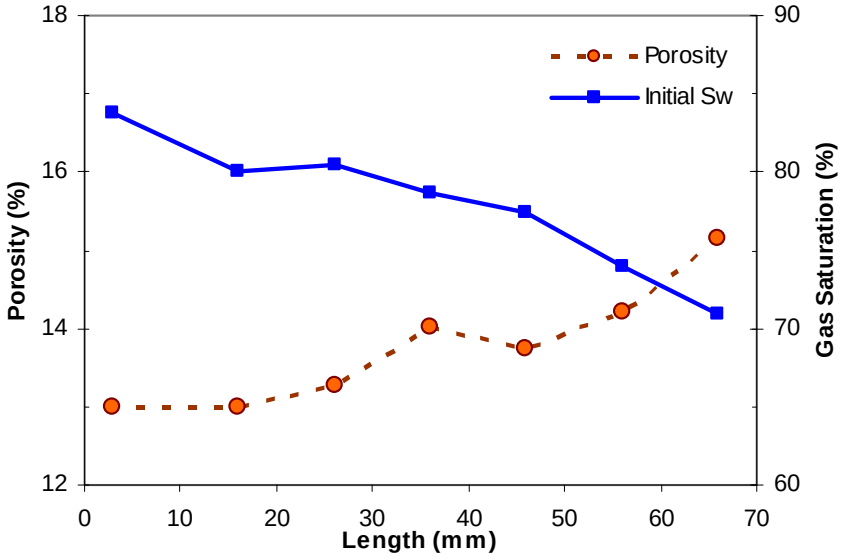

Figure 3. Porosity and saturation distribution along the length of the core calculated from CT data. Water saturation by weight 22.8 % and average water saturation by CT 22.1%.

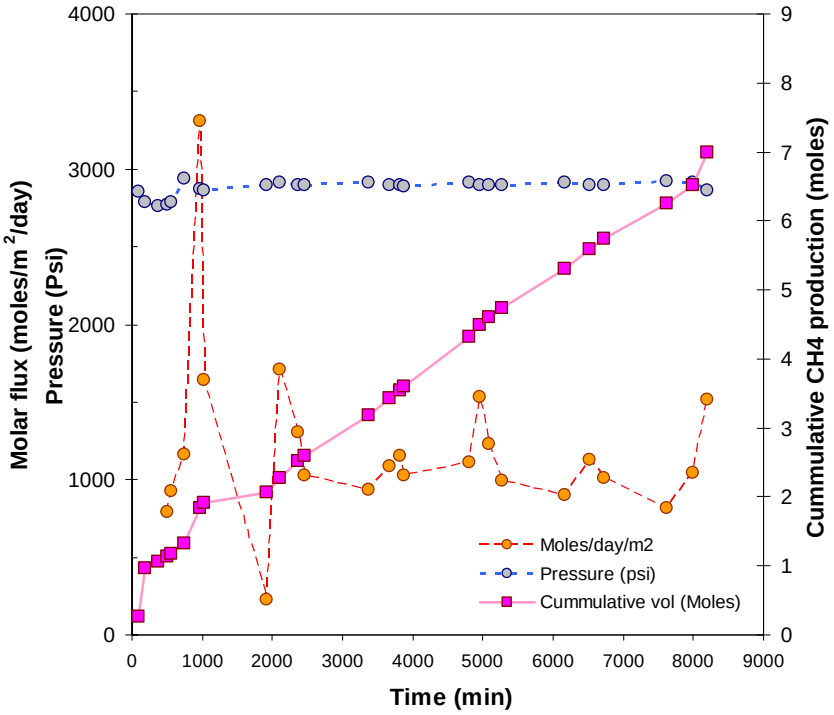

Figure 4. Methane molar flux, cumulative methane production and upstream pressure as a function of time during experiment B12.

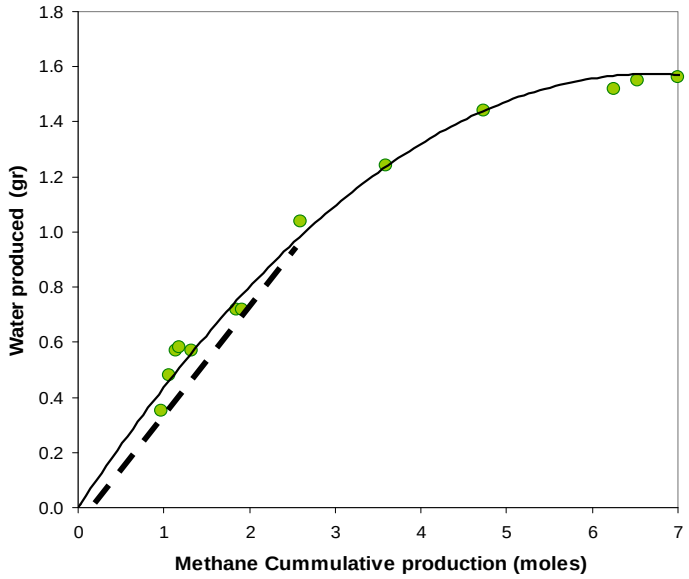

Figure 5. Water recovered from the flowing gas as a function of the molar cumulative volume during experiment B12.

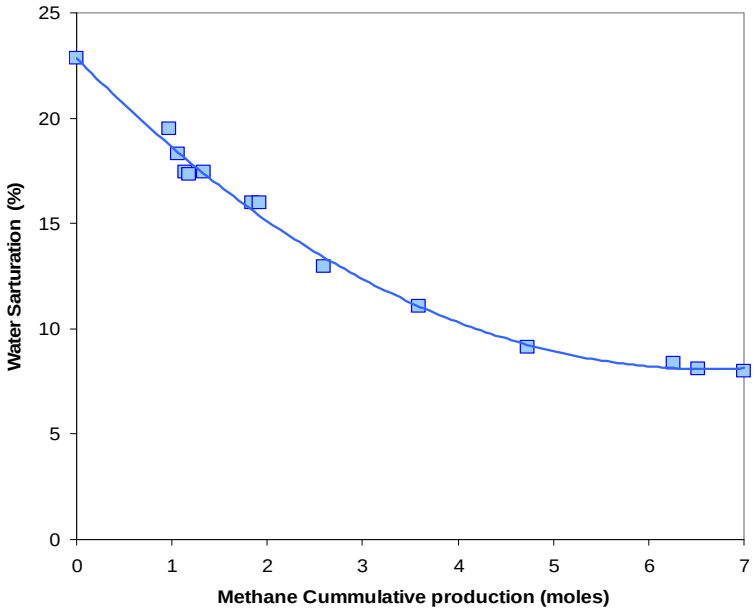

Figure 6. Approximated water saturation as a function of time during experiment B12.

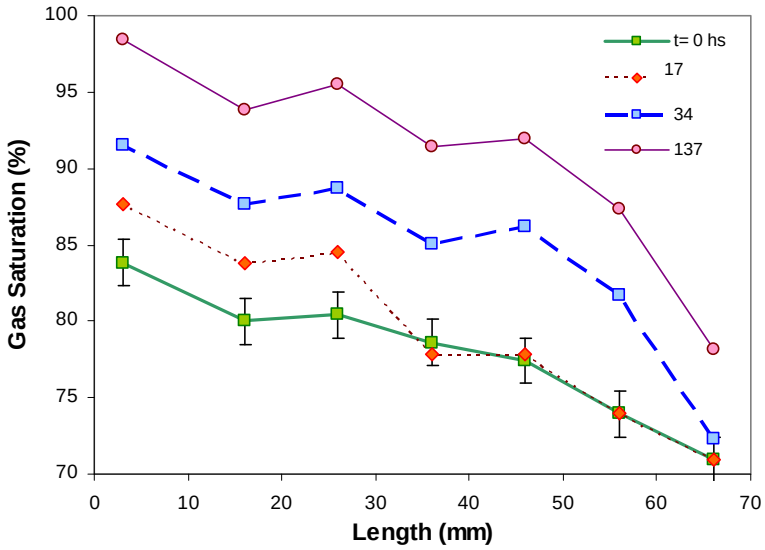

Figure 7. Saturation distribution along the core calculated from CT scanning during experiment B12. The gas saturation profile at t=0 is the same profile shown in Fig. 3 as initial Sw.

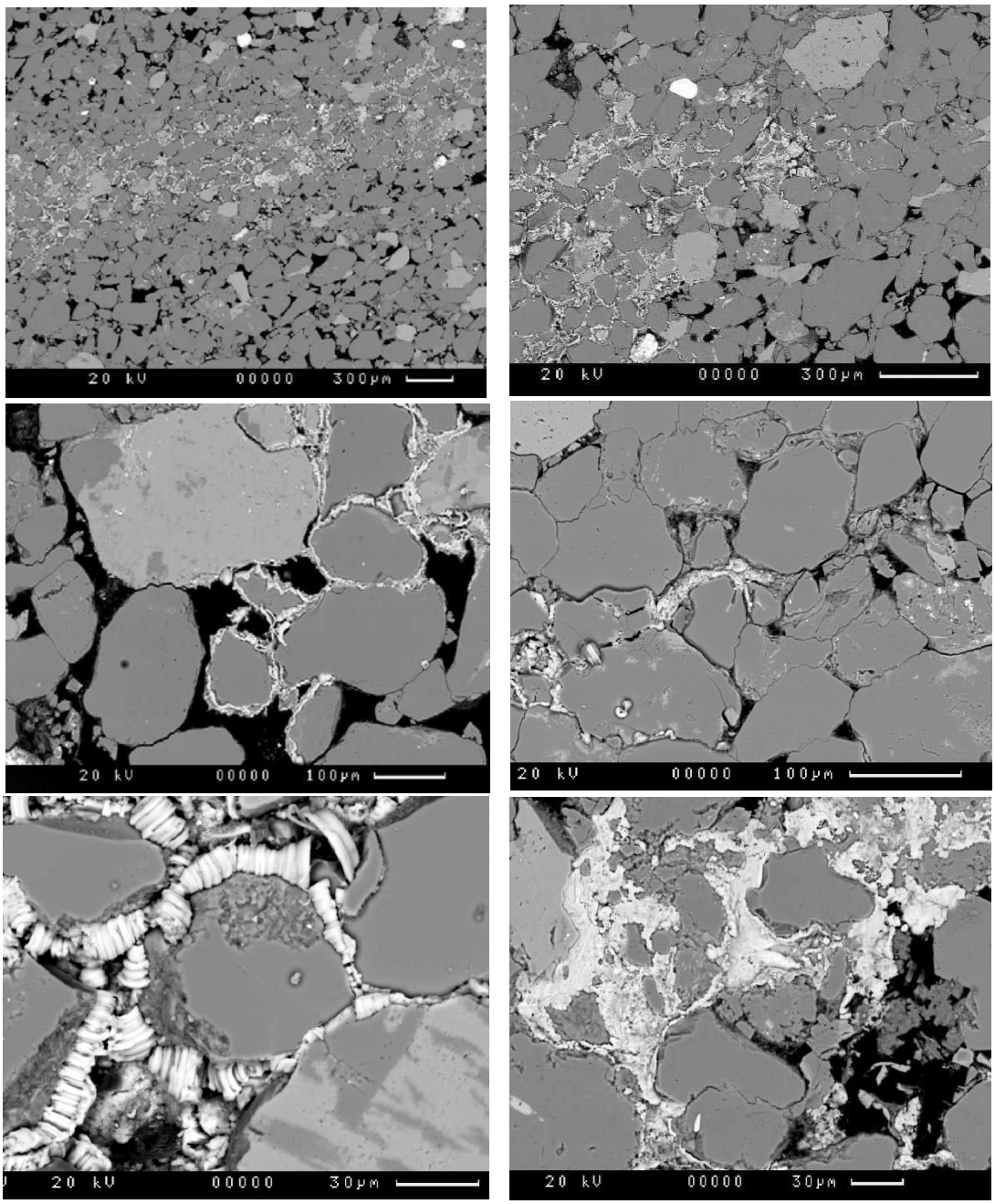

Figure 8. Backscatter SEM images of the core end face after vaporisation. The Halite appears as (bright) white to very light grey in the images, porosity is black and sand grains are grey to dark grey. Halite is mainly found in the lower permeability bands filling the smaller pores and covering the grain surface of larger pores.